JOURNAL OF MATERIALS SCIENCE **34** (1999) 795–799

Distribution of the crystal modifications in polymorphous PbSe films revealed by microhardness measurements

M. BALEVA, E. MATEEVA, E. P. TRIFONOVA
Faculty of Physics, Sofia University, 1126 Sofia, Bulgaria
E-mail: baleva@phys.uni-sofia.bg

Microhardness measurements of homogeneous and layered polymorphous PbSe films as well of the KCl and BaF_2 substrates on which the films were deposited were undertaken. The interpretation of the experimental results lead to a formula describing more adequately the indentation size effect. It is also shown that an extremum in the microhardness depth profile appears whenever the indentor crosses an interface.

1. Introduction

One of the most often measured and studied properties of thin films is microhardness. Many attempts have been made to develop more or less realistic models for interpretation of hardness tests performed on coated materials [1–3]. The restricted success of all models stems from the fact that the measured microhardness depends not only on the geometry of the indentor body and the film and substrate materials elasticity moduli, but to a great extent on the specific microstructures often obtained in thin films. Grain size, anisotropy, columnar structure, defect density, texture, layered materials and possible precipitates have to be considered when determining hardness–structure relationships.

However, in spite of the difficulties in measuring hardness values of thin films correctly, information about their specific microstructures affecting the plastic deformation processes and thus the film hardness can be obtained.

In the present work the microhardness of PbSe films deposited on two types of substrates—KCl and BaF_2, by two techniques—hot wall epitaxy (HWE) and electron beam evaporation (EBE)—is studied. The films deposited by the quasi-equilibrium HWE technique are monophase and have the stable f.c.c. NaCl-type structure [4]. The films deposited by the highly non-equilibrium EBE are polymorphous [5–7]. They consist of the three different PbSe crystal modifications—the high pressure (HP) metastable CsCl-type phase adjacent to the substrate, followed by the intermediate TlI-type phase and the stable f.c.c. NaCl-type phase as a top layer. The purpose of this work is to show that the presence of the HP metastable PbSe phases in the films grown by EBE can be identified by microhardness measurements and the distribution of the different phases across the film thickness can be followed.

2. Experiment

2.1. Samples

Microhardness measurements on PbSe films deposited by EBE and HWE were performed. The films grown by these two techniques differ in their overall crystal structure. In EBE, pairs of PbSe films were deposited simultaneously on (1 1 1) oriented BaF_2 and (1 0 0) oriented KCl substrates. The technological conditions varied in this technique are substrate temperature T_s, substrate-to-target distance L, and electron beam power E_B. It has been found that the film stoichiometry reproduces that of the target when L is about 20 cm, E_B is in the range between 100 and 300 W and T_s is maintained at different temperatures between 150 and 350 °C [8]. Our earlier structural (X-ray diffraction (XRD), reflection high energy electron diffraction (RHEED) [5, 6]) and optical (transmittance spectra [7]) investigations have shown the presence of the two HP metastable phases together with the stable phase of PbSe. The non-equilibrium technique (EBE) and the low substrate temperature provide the growth of films with the metastable phases of PbSe. The overall film crystal structure is shown in Fig. 1. The growth begins with the metastable CsCl-type phase which, at a certain thickness, turns into the intermediate TlI-type phase. The growth always ends with the formation of a sublayer of the stable phase, the thickness D_L of which depends on the evaporation time in EBE. The relative quantities of the two metastable phases grown initially depend on the substrate temperature. At low T_s the CsCl-type phase predominates, while at high T_s the TlI-type phase tends to predominate. Hence, the films represent layered structures with sublayers of different thickness and structure. The thickness D_m of the sublayers with the metastable phases has been evaluated from the modulation of the transmittance spectra of the films thicker than

0022–2461

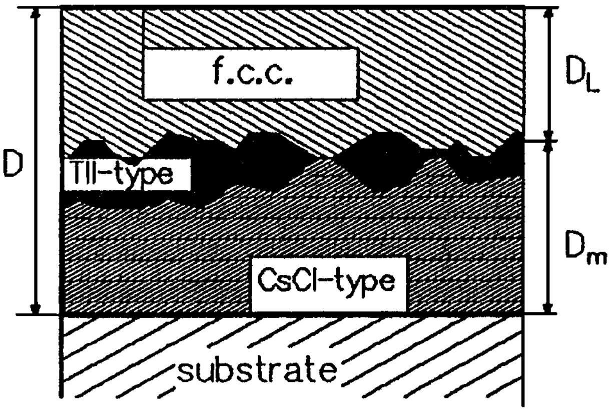

Figure 1 Schematic representation of the crystal structure over the thickness of a layered polymorphous PbSe film deposited by EBE.

2 μm. In the PbSe/KCl films $D_m \sim 1\,\mu$m, while in the PbSe/BaF$_2$ films D_m may reach 3 μm. The finding that the BaF$_2$ substrate stimulates the growth of metastable phases much more is supported by structural investigations as well [5, 6].

In contrast to the heterophase films grown by the non-equilibrium technique (EBE), the ones grown by the quasi-non-equilibrium one (HWE) are monophase. The films deposited by HWE consist of the stable f.c.c. PbSe phase alone, which is found to crystallize in the (1 0 0) direction on KCl substrates and in the (1 1 1) direction on BaF$_2$ substrates [4].

In the labeling of the samples, K stands for the KCl substrate, B - for BaF$_2$ and * marks the films deposited by HWE.

2.2. Microhardness measurements

Microhardness measurements were carried out at room temperature with the PMT-3 microhardness tester with a Vickers diamond indentor (a square based pyramid) [9]. The microhardness H is related to the load P according to the relation

$$H\left(\frac{\text{kg}}{\text{mm}^2}\right) = 1.854\frac{P(\text{kg})}{d^2(\mu\text{m}^2)}$$

and plotted as a function of the imprint diagonal d. The dependences $H(d)$ obtained are shown with points in Figs 2 to 7 as follows: in Figs 2 and 3 for the uncoated KCl and BaF$_2$ substrates, respectively; in Figs 4 and 5

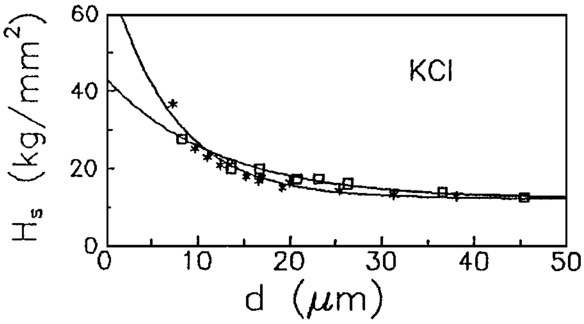

Figure 2 Microhardness depth profiles of two KCl substrates cleaved from the same bulk material. The experimentally obtained values are given with points and the lines are calculated according to Equation 2 with different values of A and D_{ps}.

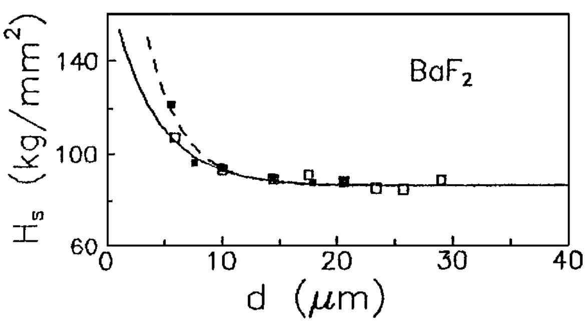

Figure 3 Microhardness depth profiles of two BaF$_2$ substrates cleaved from the same bulk material. The experimentally obtained values are given with points and the lines are calculated according to Equation 2 with different values of A and D_{ps}.

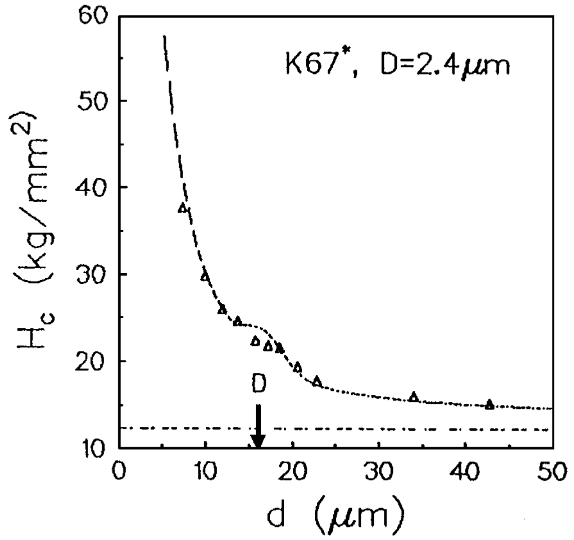

Figure 4 Microhardness depth profile of a quasi-homogeneous HWE deposited PbSe/KCl film—the experimental values are given with points and the curve is calculated according to Equation 3 with H_f and H_s from Equations 4 and 5. The value of the KCl substrate load independent hardness is shown as well.

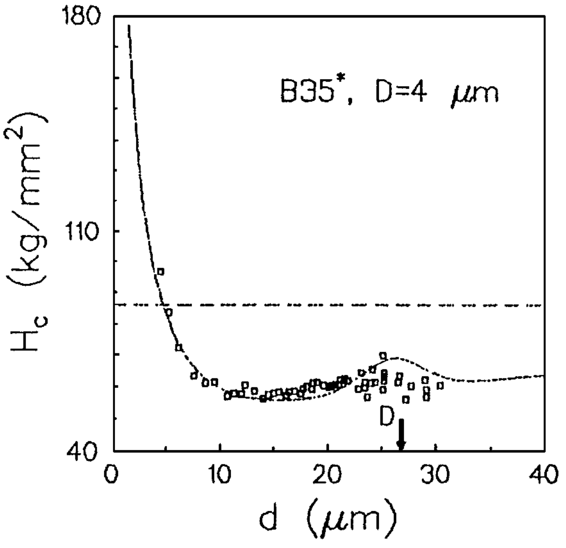

Figure 5 Microhardness depth profile of a quasi-homogeneous HWE deposited PbSe/BaF$_2$ film—the experimental values are given with points and the curve is calculated according to Equation 3 with H_f and H_s from Equations 4 and 5. The value of the BaF$_2$ substrate load independent hardness is shown as well.

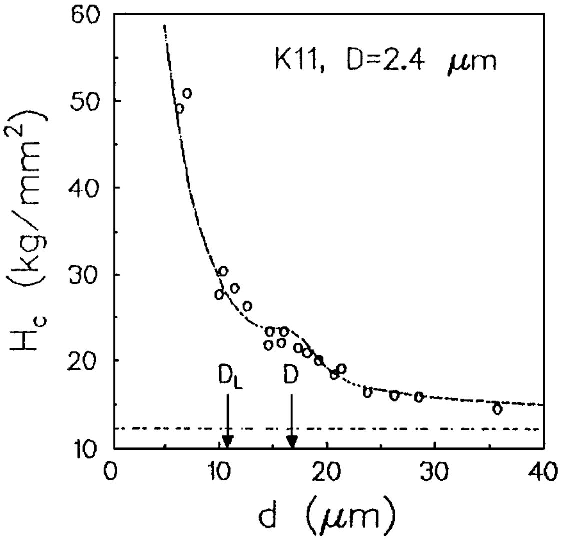

Figure 6 Microhardness depth profile of an EBE deposited PbSe/KCl film with layered polymorphous structure. The experimental values are given with points and the curve is the same as in Fig. 5 calculated with the thickness of this sample. The value of the KCl substrate load-independent hardness is shown as well.

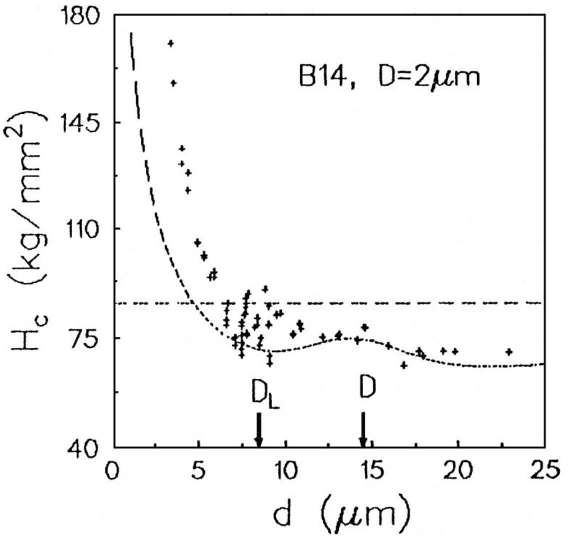

Figure 7 Microhardness depth profile of an EBE deposited PbSe/BaF_2 film with layered polymorphous structure. The experimental values are given with points and the curve is the same as in Fig. 5 calculated with the thickness of this sample. The value of the BaF_2 substrate load-independent hardness is shown as well.

for the HWE deposited PbSe films on the above mentioned substrates, and in Figs 6 and 7 for the PbSe films grown simultaneously by EBE on KCl and BaF_2 substrates, respectively.

3. Discussion

3.1. Indentation size effect (ISE)

Low loads are required for measuring the hardness of film thick only a few micrometers deposited on substrates such that the depth of indentation is only a small fraction of the total film thickness. Low loads, and thus small indentations, give rise to decreased or increased hardness values even for bulk materials. This effect is known as the indentation size effect (ISE). Several factors have been proposed to account for the ISE. Bull *et al.* [10] have demonstrated, for instance, that the effect can be due to periodic build-up and relief of the strain fields below the indentor. In general, there is enough experimental evidence to substantiate the ISE, but there is no mechanistic model to account for it. The general approach to deal with the ISE phenomenon so far has been to use Meyer's empirical law [1]:

$$H = aPd^{n-2} \tag{1}$$

where the ISE index n and the constant a are characteristics of the material being tested and the indentor geometry. When $n = 0$ there is no ISE; for $n < 2$ the hardness increases with decreasing indentation depth; for $n > 2$ the hardness decreases with decreasing indentation depth.

In Figs 2 and 3 it can be seen that the ISE really occurs even when measuring the hardness of the bulk substrate materials, KCl and BaF_2, respectively. We succeeded in fitting the experimentally measured microhardness H_s dependence on the imprint diagonal d with the function

$$H_s = H_{s\infty} + A \exp -\left(\frac{d}{D_{ps}}\right). \tag{2}$$

Here, H_s is the measured hardness of the bulk substrate, $H_{s\infty}$ is the value of the load-independent hardness of the substrate material, A is a positive or negative constant for every specific sample, characterizing the state of its surface, D_{ps} is a quantity with the meaning of deformation penetration depth, depending on the surface state, the material elastic constants and particular microstructure. In our view Equation 2 is physically more reasonable than Equation 1 as i) it involves a dimensionless coefficient $\exp -(d/D_{ps})$ and thus eliminates the uncertainty in dimensions of Equation 1, ii) involving the two independent quantities A and D_{ps} the particular properties of the surface and the volume can be accounted for more sufficiently and thus the necessity of reconsidering Meyer's law in each particular case, as for instance the Hall–Petch relation accounting for the grain size [11], can be avoided and iii) most importantly, at $d \to \infty$ the load independent hardness value $H_{s\infty}$ is reached, consistent with the experiment. In Figs 2 and 3 the experimental $H_s(d)$ dependences of two KCl and two BaF_2 substrates, respectively, are fitted with Equation 2. The fitting gives the same values for $H_{s\infty}$, but the quantities A and D_{ps} are different. The significant difference for samples cleaved even from the same bulk material indicates that these quantities are very sensitive to the state of the surface and can be regarded as empirical parameters only. The experimental $H_s(d)$ dependences fitted with Equation 2 give the following values for the load independent hardness of the substrates: KCl − $H_{s\infty} = 12.3\ \mathrm{kg\,mm^{-2}}$, BaF_2 − $H_{s\infty} = 86\ \mathrm{kg\,mm^{-2}}$. The value of $H_{s\infty}$ for KCl reported in the literature is $13.1\ \mathrm{kg\,mm^{-2}}$ [12].

3.2. Film/substrate effect

When indentation hardness tests are conducted on thin films the measurements reflect contributions from both the film and the substrate, since both deform under the indentor load. An analytical description of the individual contributions from the film and the substrate to the composite hardness would require a detailed knowledge of the elastic and plastic behavior of both the film and the substrate materials as well as of the interface characteristics and the friction between the indentor and the film. Solving this problem for the complex geometry of a square based pyramidal indentation would be an insurmountable task.

All models involve partitioning of the contributions to hardness from the substrate H_s and the film H_f in some manner. In the most general approach, proposed for instance by Buckle [13], for a film with thickness D and imprint diagonal d the composite hardness H_c of the film/substrate system is given by:

$$H_c = H_s + \alpha(H_f - H_s) \qquad (3)$$

where the coefficient alpha is supposed to depend on the film thickness. The ISE of the film/substrate system can be accounted for by writing the contribution of the film hardness by analogy to Equation 2 in the form

$$H_f = H_{f\infty} + B\exp\left(-\frac{d}{D_{pf}}\right) \qquad (4)$$

Here $H_{f\infty}$ is the value of the load independent hardness of the film material, B is a constant for every specific sample, characterizing the state of its surface, D_{pf} is a quantity with a meaning of penetration depth, depending on the state of the film surface, the film material elastic constants and particular microstructure. The parameter which influences most strongly the H_c dependence far from the surface is the load independent hardness $H_{f\infty}$ thus making possible its evaluation. The ISE can be expected to take place not only at the surface of the film/substrate system but also at the interface between the film and the substrate. This expectation is supported by the presence of a maximum in the measured composite hardness H_c at the interface, e.g. at $d = 7D$ in the case of Vickers indentor geometry. In Figs 4 and 5 it can be seen that these maxima are well pronounced both for the PbSe/KCl film with $D = 2.4\,\mu$m and for the PbSe/BaF$_2$, film with $D = 4\,\mu$m (in the figures, the thicknesses of the films are noted with arrows). Then it is reasonable to express the contribution of the substrate hardness to the measured composite hardness in the form:

$$H_s = H_{s\infty} + A^i\exp\left(-\left|\frac{d-7D}{D^i_{ps}}\right|\right) \qquad (5)$$

The quantities A^i and D^i_{ps} have to differ from the quantities A and D_{ps} in Equation 2 as A and D_{ps} characterize the penetration of the indentor from air into the substrate material, while A^i and D^i_{ps} describe the penetration from the film material into the substrate material.

The experimental dependences of H_c on the imprint diagonal d are modeled with Equation 3 in which H_f and H_s are replaced by Equations 4 and 5, respectively. In Figs 4 and 5 the calculated dependences of the PbSe/KCl and PbSe/BaF$_2$ HWE deposited films are shown with full curves. From the fitting in the case of homogeneous films deposited by HWE technique the following values for the load independent hardnesses were obtained: $H_{f\infty}^{PbSe/KCl} = 17\ \mathrm{kg\,mm^{-2}}$ and $H_{f\infty}^{PbSe/BaF_2} = 57\ \mathrm{kg\,mm^{-2}}$. These quite different values for the PbSe films deposited on the different types of substrates are not surprising as far as they refer to different crystal orientations of the stable f.c.c. phase. The films deposited on KCl substrates crystallize in the (1 0 0) direction, while those on BaF$_2$ crystallize in the (1 1 1) direction. According to Sindeeva and Godovikov [14] the microhardness of PbSe amounts to 55.5 kg mm^{-2}.

The experimental $H_c(d)$ dependences of the films deposited by EBE on KCl and BaF$_2$ substrates are shown in Figs 6 and 7, respectively. The model dependences, calculated according to Equation 3 in the homogeneous film approach are given for comparison. The thicknesses of the films D and of the upper stable phase sublayers D_L are indicated in the figures. The comparison of the experimental with the calculated curves shows: i) the films deposited by EBE are not homogeneous. The maxima at the D_L indicate the presence of an interface between the stable f.c.c. and the metastable HP phases. The latter is supported by the investigation of a number of thicker films, the maxima in the $H_c(d)$ dependences of which indeed appear at the interface between the two sublayers whose thicknesses we have been able to evaluate from the modulation of their interference spectra. It is worth pointing out that the experiment supports our earlier finding that the sublayers with the HP phases are thicker in the films deposited on BaF$_2$ than those deposited on KCl substrates. In the two PbSe films deposited simultaneously on KCl (K11) and BaF$_2$ (B14), $D_m \sim 0.8\,\mu$m for PbSe/KCl films and $D_m \sim 1\,\mu$m for PbSe/BaF$_2$ films; ii) The films deposited by EBE show higher values of the measured composite hardness H_c. It can be expected that the load independent hardness of the HP metastable phases is higher than the hardness of the stable phase. However, in the case of such thin films with two or even three relatively well-defined sublayers (stable + TlI-type + CsCl-type phases) the increase in H_c is rather due to the layered structure, i.e. to the increase of the hardness at the interface between the different phases. The maxima in the microhardness depth profiles due to the indentor crossing the interfaces f.c.c./TlI-type phases and TlI-type/CsCl-type phases cannot be resolved as the intermediate sublayer with the TlI-type phase, even though well-defined, is thin. These maxima coalesce to give rise to an increase of the microhardness in a broad range.

4. Conclusion

From the experimental investigation of the microhardness and our attempts adequately to interpret the experimental results, the following conclusions can be drawn:

- It is physically more reasonable to describe the ISE by an exponential dependence rather than by Meyer's law.

- The ISE has to be taken into account not only at the surface of the film/substrate system but at all interfaces as well. The presence of interfaces leads to an increase of the measured hardness H_c, e.g. to the appearance of maxima in it. Thus, from the microhardness measurements the thicknesses of the different sublayers of a layered structure can be evaluated.

References

1. P. J. BURNETT and D. S. RICKERBY, *Thin Solid Films* **148** (1987) 51.
2. P. J. BURNETT and T. F. PAGE, *J. Mater. Sci.* **19** (1984) 845.
3. B. JONSSON and S. HOGMARK, *Thin Solid Films* **114** (1984) 257.
4. M. MAKSIMOV, *Bulg. J. Phys.* **12** (1985) 3.
5. M. BALEVA and E. MATEEVA, *J. Phys. Condens. Matter.* **5** (1993) 795.
6. M. BALEVA and E. MATEEVA, *J. Mater. Sci. Lett.* **14** (1995) 258.
7. M. BALEVA, E. MATEEVA and M. MARINOV, *ibid.* **14** (1996) 167.
8. E. MATEEVA, M. MAKSIMOV, V. VULCHEV and YU. BESSEDIN, Proceedings of the First General Conference of the Balkan Physical Union, September 26–28, 1991, Thessaloniki, Greece, edited by K. Paraskevopoulos **2** (1991) 715.
9. N. A. GORYUNOVA, A. S. BORSHEVSKII and D. N. TRETIAKOV in *Semiconductors and Semimetals*, edited by R. K. Willardson and A. C. Beer. Vol. **4** (Academic Press, New York, 1968) 3.
10. S. J. BULL, T. F. PAGE and E. H. YOFFE, *Philos. Mag. Lett.* **59** (1989) 281.
11. P. HAASEN, in "Physical Metallurgy," (Cambridge University Press, Cambridge, 1978) 151.
12. P. SUPTITZ and J. TELTOW, *Phys. Stat. Solidi.* **23** (1967) 9.
13. H. BUCKLE, in "The Science of Hardness Testing and its Research Applications," edited by J. W. Westbrook and H. Conrad (American Society for Metals, Metals Park, OH, 1973) 453.
14. N. D. SINDEEVA and A. A. GODOVIKOV, *Dokl.* **127** (1959) 431.

Received
and accepted